Test-station for flexible semi-automatic wafer-level silicon photonics testing

J. De Coster, P. De Heyn, M. Pantouvaki,
B. Snyder, H. Chen, E. J. Marinissen,
P. Absil, J. Van Campenhout
3D and optical I/O technologies
imec
Heverlee, Belgium
jeroen.decoster@imec.be

B. Bolt
Systems BU
Cascade Microtech, Inc.
Beaverton, OR, USA

***Abstract*—Silicon photonics technologies are a particularly attractive solution for developing low-cost optical interconnects with high performance. Imec is developing a silicon photonics technology platform. Developing this platform requires continuous process optimization and design verification, both of which are enabled by the flexible wafer-level test solution that is presented in this paper. The test station enables semi-automatic optical and electro-optical testing of passive and active silicon photonics components and circuits, including waveguides, fiber grating couplers, photodetectors, modulators, filters etc. The measured insertion loss of fiber grating couplers is repeatable to within 0.07dB (6σ), for photodetector responsivity the repeatability is around 0.02A/W (6σ). Calibration procedures have been designed to ensure the long-term reproducibility of measurement results. This is demonstrated with wafer-level measurement data for fiber grating couplers and photodetectors that were gathered over a five-month period. The repeatability over this period is 0.8dB for the insertion loss and 0.09A/W for the responsivity measurement.**

Keywords—silicon photonics, optical interconnects, wafer-level testing

I. INTRODUCTION

As the need for data links with ever greater bandwidth continues to grow, optical interconnects are becoming an attractive alternative to electrical links. The cost and performance of optical transceivers are key elements that determine the economic viability of optical interconnects. Imec is addressing these two elements by developing an active silicon photonics platform that leverages existing CMOS infrastructure and processing techniques to provide a wide range of passive and active optical devices on silicon wafers [1], [2]. Developing the specific process modules for this photonics platform, as well as establishing a component library with predictable, stable, and reliable device performance requires efficient wafer-level testing capabilities to provide accurate feedback regarding device performance to process engineers and optical component and circuit designers.

Wafer-level photonics testing hardware is, just like the silicon photonics technology itself, a newly emerging application for manufacturers of test equipment. Die-level testing has been enabled by the use of edge coupling [3], as used e.g. in the I/O front-end test station presented in [4]. The use of diffractive gratings for coupling photonic waveguides with single-mode fibers (SMF) is becoming an established technique that enables photonic circuit packaging and wafer-level testing [5], [6], [7]. Others have suggested the use of special optical probes rather than fibers [8]. In this paper we present a highly flexible test setup that is based on a standard 300mm probe station for semiconductor characterization. The motorized fiber manipulators allow to measure any combination of optical and electrical ports of photonics circuits with highly customized layouts as schematically depicted in Fig. 1.

The test station allows to characterize both passive and active photonics devices. For passive devices such as fiber grating couplers (FGC), waveguides and filters, the optical transmission spectrum can be measured in the O- (1260-1360nm), C- (1530-1565nm), and L- (1565-1625nm) bands. For active devices such as photodiodes and modulators, electrical and electro-optical parameters can be measured as well. Electrical measurements can be performed at DC (IV measurement, photocurrent measurement, diode responsivity) as well as at RF frequencies (e.g. detector and modulator bandwidth). Moreover, an optical calibration method has been developed and the repeatability of measurement data is being actively monitored.

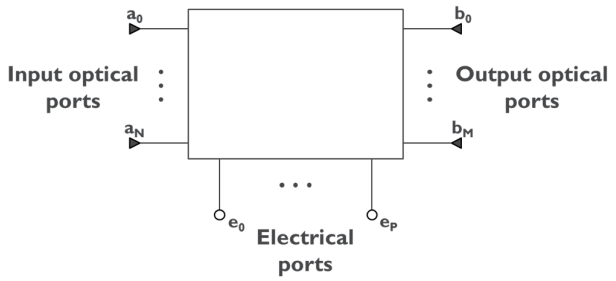

Fig. 1 Photonics circuit featuring several optical input and output ports, as well as multiple electrical contact pads.

978-1-4673-9659-2/16/$31.00 ©2016 IEEE

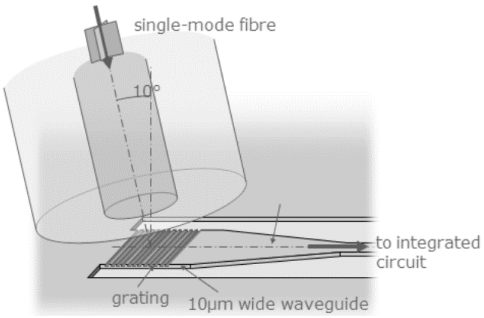

Fig. 2 SM fiber positioned above a FGC. The fiber is held at a 10° angle from vertical [5].

The paper is organized as follows: an introduction to the use of diffractive gratings for wafer-level testing is given in Section II. Section III gives an overview of the hardware components that are used in the test setup. The baseline measurement flow is then highlighted in Section IV, where special emphasis is laid on the automatic fiber alignment procedure. Extensive wafer-level measurement results and setup stability monitoring results are presented in Section V. Finally, the concluding remarks are given in Section VI.

II. Wafer-Level Testing of Optical Components

Performing optical tests at wafer level requires a method of coupling light from an optical fiber into the optical circuits on the wafer, and vice versa. The approach that is adopted in this work consists of positioning a SMF almost perpendicular to the surface of the wafer above a fiber grating coupler (FGC) on the wafer to collect and channel the light into a waveguide on the wafer. This is schematically depicted in Fig. 2. As such, the FGC is the workhorse for wafer-level optical and electro-optical testing and characterizing the FGC's performance is therefore of paramount importance. Since the mode field diameter (MFD) of the SMF is 10.2µm at 1550nm and the width of the FGC is about 10µm, a precise alignment of the fiber to the FGC is required in order to get efficient coupling. Typically, 2µm lateral misalignment results in a 1dB increase of the optical insertion loss [4] whereas only about 0.1dB uncertainty on the coupling efficiency can be accepted during measurements. Sub-micron alignment accuracy is therefore required. Section IV.C is dedicated to a discussion of the automatic fiber alignment routine that is implemented in the test station.

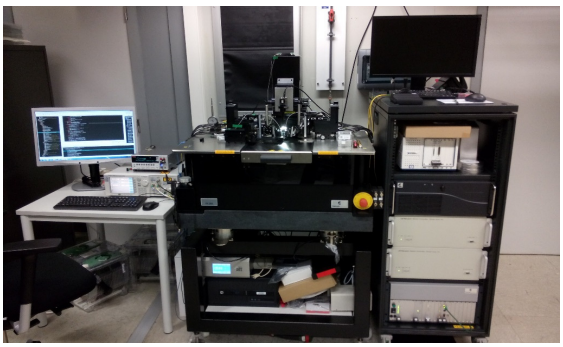

Fig. 3 Photograph of the test station.

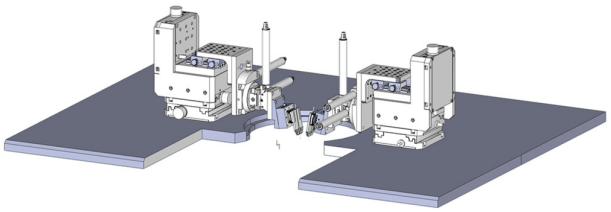

Fig. 4 Schematic drawing of the two motorized fiber manipulators in an east-west arrangement on the prober's platen.

III. Test Station Hardware

This section gives an overview of the hardware components that are present in the test station. A photograph of the setup is shown in Fig. 3.

The system is built around a semi-automatic 300mm probe station. The prober is equipped with one RF probe manipulator and two custom-made motorized fiber manipulators. The fiber manipulators are arranged in an east-west layout as depicted in Fig. 4, the RF probe is mounted either in the north or south position.

Each of the fiber manipulators is designed with six motorized degrees of freedom (DOF): translation in x, y, z and yaw, pitch, roll adjustment. Positioning resolution amounts to 10nm for the translation stages and 12 arc sec for the rotation stages.

Fig. 5 illustrates the optical configuration of the measurement setup. The optical instrumentation consists of two tunable laser sources covering the O-band and the C- and L-band, an optical power meter and a polarization controller. Single-mode fibers with angled physical contact (APC) connectors are used in the optical path. As depicted in Fig. 2, the light is coupled with the FGC on the device wafer using bare SMF that are terminated with a straight cleaved facet. These fibers are called the 'measurement pigtails'. Electrical instrumentation consists of a source-measure unit (SMU) and a lightwave component analyzer (LCA) which allows measuring S-parameters up to 50GHz in the electrical and electro-optical domains.

IV. Test Sequence

The basic measurement procedure for optical and electro-optical measurements is illustrated in Fig. 6. Each of the main steps in this baseline measurement flow will be described in the following paragraphs.

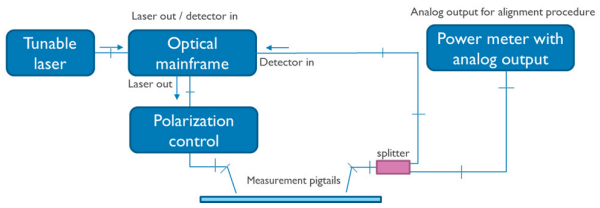

Fig. 5 Schematic overview of measurement setup.

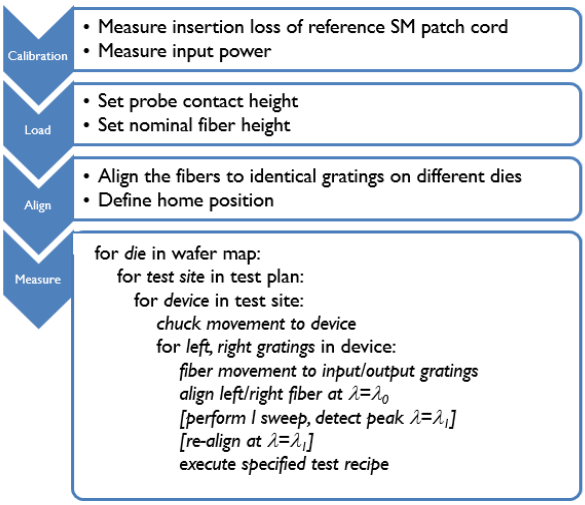

Fig. 6 Baseline optical and electro-optical measurement procedure.

A. *Optical calibration*

The first step is an optical calibration step, during which the optical losses in all components (patch cords and sleevethrough connectors, polarization controller, optical splitters) of the setup are characterized over the full wavelength span of the tunable laser source(s). This is accomplished by bypassing the two measurement pitgtails using a reference patch cord. The recorded spectrum (shown as the bottom curve in Fig. 7) is stored and used for correcting all wafer-level measurement data. This is illustrated in Fig. 7 for a measurement on a short waveguide with an input and output FGC: after subtracting the setup loss spectrum, the actual insertion loss of the grating structure is obtained. The fiber-to-wafer insertion loss (FtW IL) is then defined as half of the loss of this test structure.

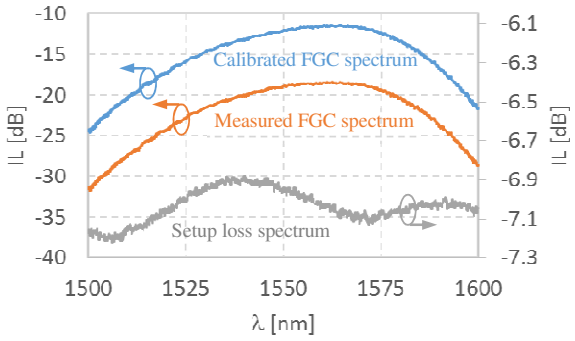

Fig. 7 Measured spectra: optical losses in the setup (secondary vertical axis), raw FGC spectrum (primary vertical axis) and calibrated FGC spectrum (primary vertical axis).

The second part of the calibration step consists of measuring the optical power at the tip of the input measurement pigtail using a free-space detector. After subtracting the FtW IL for a given FGC, one obtains an accurate estimate of the absolute optical power reaching the DUT on the wafer. This is of particular interest e.g. for photodiode responsivity measurement.

B. *Loading the wafer*

When a wafer is loaded, the probe contact height is defined as well as the fiber tip height. The importance of maintaining a constant fiber tip height throughout a wafer-level measurement run is illustrated in Fig. 8. The figure shows the FtW IL of a FGC, measured at different fiber heights on 14 die locations that were spread evenly across the wafer (i.e. both center die and edge die locations are included). It is observed that the FtW IL varies with fiber tip height by about 0.05dB/µm. As a consequence, fiber tip height needs to be verified and defined at the home position for each measurement run in order to obtain consistent measurement data.

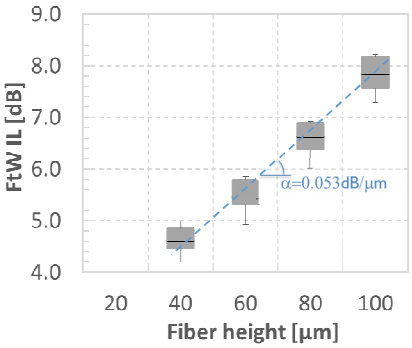

Fig. 8 Measured fiber-to-wafer insertion loss (FtW IL) on a set of 14 die locations, at several heights of the fiber tip above the wafer surface.

Moreover, the above observation implies that any non-planarity of the wafer chuck will strongly affect the measurement results. The chuck topography was therefore measured using a digital micrometer gauge and the measured data points were stored in a lookup table. When executing a measurement sequence, the fiber height is adjusted by interpolation in this table. The impact on measured FtW IL for the grating data from Fig. 8 is shown in Fig. 9.

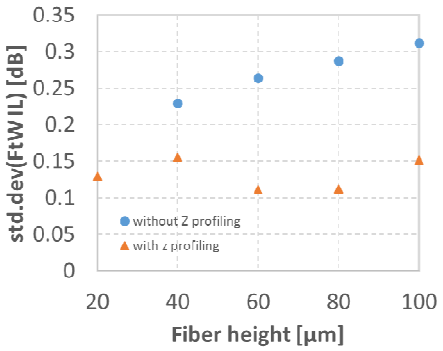

Fig. 9 Reduction of spread on the measured FtW IL by implementing the chuck topography compensation.

C. *Fiber alignment*

Once the wafer is aligned and the home position has been defined, the actual test sequence is executed. The main difference in comparison with standard electrical testing is the fiber alignment step that occurs before each measurement. After the fibers have moved to the destination input and output FGC,

an automatic fiber alignment routine is executed. Optionally, a wavelength sweep is performed after fiber alignment and the fibers are then re-aligned at the detected peak wavelength.

During fiber alignment, the measurement pigtail moves along a pre-defined trajectory in (x,y). While the fiber moves, the transmitted optical power p_i is recorded. At the same time, the stage positions are read from the stage encoders. The resulting data set of (x,y,p_i) samples is then fitted with an analytical expression in order to obtain the (x_c,y_c) coordinate of the location with optimum coupling efficiency.

In some cases, it may be required to perform a wavelength sweep at this point, determine the wavelength with peak transmission, and re-align the fibers at the peak wavelength (e.g. when measuring filters or modulators). In those cases, the re-alignment is performed with a reduced travel range of the fiber tip in order to save time.

For active devices such as photodetectors, an alternative fiber alignment method has been implemented where the photocurrent i_p is monitored rather than the transmitted optical power. The (x,y,i_p) data set is then processed in exactly the same manner in order to determine the optimum fiber position.

D. Execution of the measurement recipe

When the fibers have been aligned, a device-specific test recipe is executed. The extensive library of test recipes includes the following: (1) loss measurement, i.e. measurement of optical insertion loss while sweeping wavelength, (2) detector measurement, i.e. measurement of IV with and without light, measurement of photocurrent versus wavelength, (3) modulator measurement, i.e. measurement of IV and measurement of optical insertion loss versus wavelength at different bias voltages, (4) S parameter measurement, i.e. measurement of purely electrical or electro-optical S parameters while varying DC bias and/or wavelength.

V. Wafer Level Measurement Results and Assessment of Setup Stability

In the previous section, several improvements to the robustness of the measurement flow were discussed, leading to a reduction of the spread of the measured quantities. Consistency among data sets is indeed a major concern when comparing data from wafer to wafer or from lot to lot, as SMF interfaces are known to be sensitive to environmental influences. In order to verify the performance of the measurement setup, a dedicated reference wafer is being measured at regular intervals and a number of device parameters are tabulated such that inconsistencies can be detected and corrected. Measurement results from this reference wafer are presented in this section and both the short-term and long-term repeatability are assessed.

A. Short-term repeatability

In a first set of experiments, the reference wafer was repeatedly measured at 30 minute intervals. Two types of FGCs and one type of photodiode were measured on the same set of 14 die locations as shown in Fig. 8. The fiber tip height was set to 20µm at the center die and chuck topography compensation was enabled. From these measurements, the FtW IL and the detector responsivity were calculated.

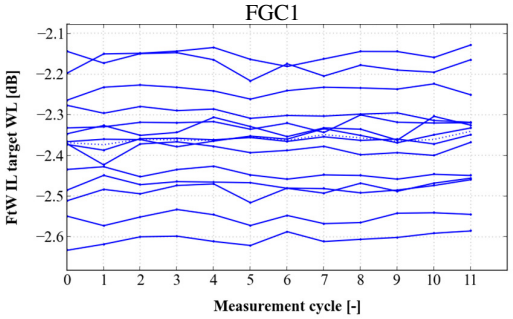

Fig. 10 Measured coupling efficiency on a set of 14 die locations across the reference wafer.

Fig. 10 shows the measured coupling efficiency over 12 test cycles, one trace in the figure represents the measurement data from one die. The repeatability of the measurement result for a die location is defined as the standard deviation of all the measured coupling efficiency values for this die. The average repeatability for the 14 die locations from Fig. 10 amounts to 0.012dB. Similarly, the repeatability of the measured photodetector responsivity is found to be 0.0038A/W.

B. Long-term reproducibility

Over the longer term, the measurement setup is subject to various uncontrolled influences: the facets of the measurement pigtails are subject to contamination, mechanical alignment of components can change due to changes in ambient temperature, polarization of the incoming light can change due to movements of the SMF, the insertion loss of sleevethrough connectors is subject to some variability whenever patch cords are disconnected, etc. In order to capture these effects, the reference wafer is measured on a regular basis. Fig. 11a shows the measured FtW IL for the same FGC ('FGC1') and the same die locations as presented in Fig. 10, over a period of about 5 months. Defining the reproducibility as the standard deviation of data points for a given die location, the reproducibility $\Delta_{FtW\,IL}$ of the FtW IL over 5 months amounts to 0.14dB. Results for another type of FGC ('FGC2') are shown in Fig. 11b. The reproducibility for FGC2 is around 0.18dB.

The graph in Fig. 11c shows the measured responsivity of a waveguide-coupled photodetector ('GePD', [9]) that is coupled using FGC2. The responsivity R of photodetectors is related to FtW IL according to (1):

$$R = 10^3 I_p 10^{(FtW\ IL - P_l)/10} \tag{1}$$

Where P_l is the absolute power of the laser light that is incident on the FGC and I_p is the measured photocurrent. The contribution of $\Delta_{FtW\,IL}$ to the reproducibility of the detector responsivity can thus be estimated as follows:

$$\Delta_R = \frac{\partial R}{\partial FtW\ IL} \cdot \Delta FtW\ IL \tag{2}$$

For the photodetector from Fig. 11c, this expression evaluates to $\Delta_r = 0.019$A/W – compared to a value of 0.016A/W that is observed in the responsivity measurement data. As such, we speculate that the variability in the responsivity measurement originates mostly in the variability of the coupling efficiency, and that other contributions are negligible.

C. Discussion

The observations from Sections A and B indicate that the long-term reproducibility of the measurement data is five to ten times greater than the short-term repeatability. Factors that influence the repeatability include the positioning accuracy of the measurement pigtails, the readout accuracy of the power meter, variation in probe-to-pad resistance, and accuracy of the photocurrent readout for detector measurements.

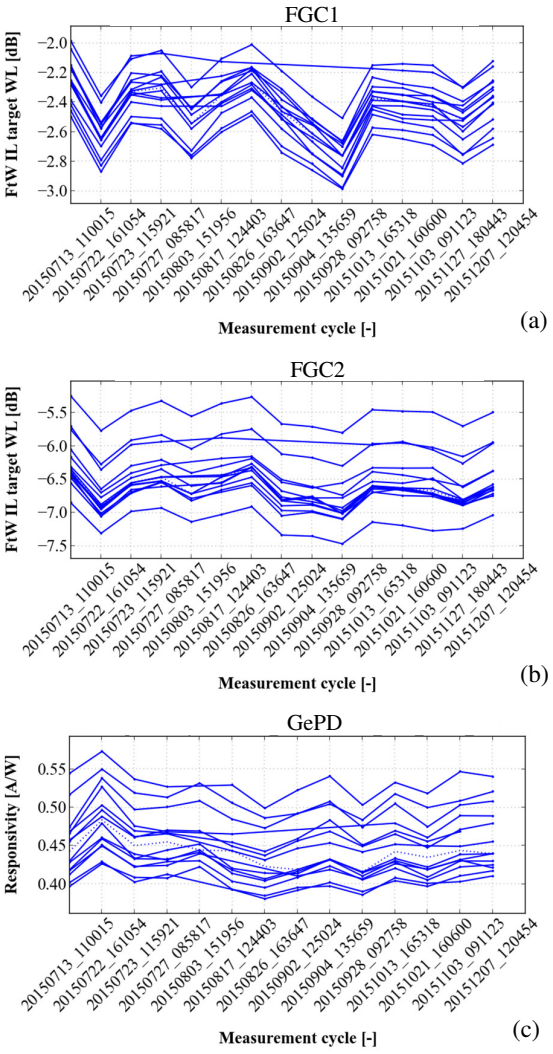

Fig. 11 Measured FGC coupling efficiency and photodetector responsivity over a period of 5 months.

Given this large difference between the repeatability and reproducibility, the long-term reproducibility does not seem to be dominated by these factors. The graphs from Fig. 11 also show very consistent trends when comparing different die locations, which suggests that the long-term accuracy of the measurement is dominated by a systematic drift in the setup's performance. This is why the calibration procedure from Section IV.A has been implemented and graphs like those shown in Fig. 11 are being used in order to determine when corrective actions are needed (e.g. clean or replace measurement pigtails, check sleevethrough connectors for dust particles). The reproducibility of measurement results can be further improved by performing this reference measurement at shorter intervals and promptly carrying out corrective actions. The latter is especially important in order to bring the reproducibility numbers further down.

VI. Conclusions

A test station for semi-automatic wafer-level characterization of silicon photonics devices has been developed. Several features have been implemented that are aimed at optimizing the accuracy and reproducibility of the measurement results. The fiber alignment routine leads to a robust fiber alignment with less than 0.07dB (6σ) variability in the measured fiber-to-wafer insertion loss. Topography of the wafer chuck is being compensated for, resulting in a 35% reduction of the within-wafer spread of the FtW IL at 40µm fiber height. A reference wafer is being periodically monitored; over a five-month period this gave a reproducibility of better than 0.8dB in insertion loss and 0.09A/W in photodetector responsivity (6σ).

Acknowledgment

The authors acknowledge imec's 200mm and 300mm pilot line for contributions to the device fabrication and imec's PDK team for mask preparation and tape-out. This work was supported by imec's Optical I/O Industrial Affiliation Program.

References

[1] P. Absil, P. De Heyn, H. Chen, P. Verheyen, G. Lepage, M. Pantouvaki, J. De Coster, A. Khanna, Y. Drissi, D. Van Thourhout, J. Van Campenhout, "Imec iSiPP25G silicon photonics: a robust CMOS-based photonics technology platform", SPIE Photonics West 2015

[2] M. Pantouvaki, P. De Heyn, M. Rakowski, P. Verheyen, B. Snyder, S. A. Srinivasan, H. Chen, J. De Coster, G. Lepage, P. Absil and J. Van Campenhout, "50Gb/s Silicon Photonics Platform for Short-Reach Optical Interconnects", Optical Fiber Communication Conference and Exposition 2016, accepted for publication.

[3] B. Ben Bakir, A. V. de Gyves, R. Orobtchouk, P. Lyan, C. Porzier, A. Roman, J.M. Fedeli, "Low-Loss (1 dB) and Polarization-Insensitive Edge Fiber Couplers Fabricated on 200-mm Silicon-on-Insulator Wafers", *Photonics Techn. Letters, IEEE* , vol.22, no.11, pp.739-741, June1, 2010

[4] D. Watanabe, S. Masuda, H. Hara, T. Ataka, A. Seki; A. Ono, T. Okayasu, "30-Gb/s optical and electrical test solution for high-volume testing", *Test Conference (ITC), 2013 IEEE International* , pp.1-10, 6-13 Sept. 2013

[5] D. Taillaert, W. Bogaerts, P. Bienstman, T.F. Krauss, P. Van Daele, I. Moerman, S. Verstuyft, K. De Mesel, R. Baets, "An Out-of-Plane Grating Coupler for Efficient Butt-Coupling Between Compact Planar Waveguides and Single-Mode Fibers", IEEE Journal of Quantum Electronics, vol. 38(7), pp.949-955, 2002.

[6] G. Roelkens, D. Vermeulen, F. Van Laere, S. Selvaraja, S. Scheerlinck, D. Taillaert, W. Bogaerts, D. Van Thourhout, R, Baets, "Bridging the Gap Between Nanophotonic Waveguide Circuits and Single Mode Optical Fibers Using Diffractive Grating Structures", Journal of Nanoscience and Nanotechnology, vol. 10, pp. 1551-1562, 2010

[7] T. Horikawa, D. Shimura, J. Seok-Hwan, M. Tokushima, K. Kinoshita, T. Mogami, "Process control and monitoring in device fabrication for optical interconnection using silicon photonics technology", *Interconnect Technology Conference and 2015 IEEE Materials for Advanced Metallization Conference (IITC/MAM),* pp.277-280, 18-21 May 20, 2015

[8] R.R. Panepucci, A.J. Zakariya, L.V.K. Kudapa, "Flexible waveguide probe for silicon-photonics wafer-level test", *Microwave & Optoelectronics Conference (IMOC), 2011 SBMO/IEEE MTT-S International* , pp.111-113, Oct. 29 2011-Nov. 1 2011

[9] H. T. Chen, P. Verheyen, P. De Heyn, G. Lepage, J. De Coster, P. Absil, G. Roelkens, J. Van Campenhout, "High-Responsivity Low-Voltage 28-Gb/s Ge p-i-n Photodetector With Silicon Contacts", *Lightwave Technology, Journal of* , vol.33, no.4, pp.820-824, Feb.15, 15 2015